Dispersion of VOC vapours in the surface treatment workspace: influence of variability in diffusivity, mass transfer and air velocity.

V. Hilborne[1*] and A.F. Averill[2]

[1]School of Applied Science. [2]Chemical Engineering Research Centre. London South Bank University, London SE1 0AA UK.

Abstract

Wherever solvents are allowed to disperse into the workspace it is necessary to be able to predict and determine their concentration and the effect of air velocity variations. Models developed to predict dispersion for assessing ventilation efficiency and worker exposure are validated against measured data with varying success. In numerical convection - dispersion models, including computational fluid dynamics (CFD) methods, the transport coefficient effective diffusivity is used as a turbulence closure parameter and air velocities are used to define convective mass transport. This study shows how transport coefficient values, empirically estimated from airborne volatile organic carbon (VOC) vapour concentrations from a solvent source, vary in a ventilated workspace. Variability in effective diffusivity values demonstrates non-Fickian dispersion from the source along the length of a one dimensional axis. An important finding was that a correlation between air velocity and vapour transport data was not found. This suggests that air velocity should not be used a-priori to represent mass transport in the determination of vapour dispersion in the workplace.

Keywords: Surface treatment workspace, Organic vapours, Effective diffusivity, Mass transport coefficient, Air velocity

Introduction

Solvent degreasing remains a widesprad operation in the metal finishing industries and although many of the traditional open topped tanks that used organic solvents have now been replaced by enclosed plant, some traditional plant and organic solvents are still in use[1] . Even in the case of closed systems, exposure risk needs to be assessed during periods of equipment maintenance. **As a result of the Montreal Protocol in 1987[2] , much effort was made (e.g.** Averill et al.[3-5]) to find effective cleaning agents that were acceptable alternatives to solvents such as 1,1,1 trichloroethane (TCA),1,1,2-, trichlorotrifluoroethane (CFC-113), and methyl chloroform. Whilst trichloroethylene, another widely used solvent, satisfies the environmental requirements, having zero ozone depletion and global warming potential, it is seriously injurious to health and is assigned, under Schedule 2A of COSHH[†], the risk phrase

* Corresponding author, email hilborv.lsbu.ac.uk
† Control of Substances Hazardous to Health

R45. Under the current system (REACH[‡1, 6, 7]) that regulates the use of organic solvents in the EU, trichloroethylene will require authorisation after April 2016 for its continued use. From that date it is unlikely to be used in any un-enclosed degreasing system.

Although the move towards closed ventilation systems has reduced consumption of volatile organic carbon (VOC) solvents, ventilation to negate operator exposure to VOC's during cleaning, maintenance or from open processes is essential. Whatever solvent or solvent system is used, it will be necessary to determine its concentration in the workspace and to understand the controlling factors. In addition, ventilation efficiency and occupational exposure need to be risk assessed and monitored.

Averill et al[8, 9] carried out a study to investigate the evaporation and dispersion of replacement solvents, HFE and HFC based azeotropes and n-propyl bromide (nPBr) during wipe cleaning of metal components. The volatility of the solvent system clearly has a great bearing on the occupational health hazard to operatives as well as on the cost of the cleaning process. It was shown that the azeotropic solvents evaporated at rates comparable to or less than CFC-113 whilst nPBr evaporates at a rate similar to TCA. In the second part of the study[9] a Monte Carlo uncertainty analysis using a diffusion based exposure assessment model was employed to aid forecasting of solvent vapour concentrations in the workspace during wipe cleaning of metal components. After selecting a reasonable range for each variable inputted to the spherical diffusion equation, randomly selected values were introduced into the equation enabling the distribution of solvent vapour concentration to be obtained. Since diffusion in the workspace is mostly brought about by the turbulent motion of the air rather than by molecular diffusion, this is taken into account by defining an eddy diffusivity term which combines the influence of both processes. With the spherical diffusion model, solvent vapour is emitted from a continuous point source so that initially an envelope of vapour will form around the source which expands outwards with time. This movement will at first be rapid, slowing later until the expansion ceases. At this point, the total rate of loss of solvent vapour through its surface becomes equal to the rate of generation of the vapour at the source. It was recognized that a major practical difficulty is to establish an appropriate value for the eddy or effective diffusivity that will provide realistic prediction of the movement of the vapour cloud and distribution of vapour concentration with time.

[‡] Registration, Evaluation, Authorisation and Restriction of Chemicals

Prediction models have continued to be developed to define dispersion of airborne contaminants from single or multiple sources for occupational health assessment, hazard mitigation and ventilation design. These models reduce the need for expensive, time consuming systems of measurement and aids interpretation of the physical processes that drive dispersion. The numerical convection (or advection) – diffusion equation forms the basis for dispersion modelling in both the large scale atmosphere and small indoor spaces including industrial workplaces. Computational fluid dynamics (CFD) methods are examples where convection – diffusion is interpreted through the Navier-Stokes equations. CFD models can provide detail in spatial distribution and evolution of contaminants over time and are generally more successful when fine spatial grids and small time steps are used. Fine grids however demand greater computational resources. Numerical methods are also vulnerable to numerical dispersion and error amplification so require flux corrective schemes such as those described by Rood[10] and Emmerich and McGrattan[11]. Many workers such as Kassomenos et al.[12] and Zhang et al.[13] used $k - \varepsilon$ CFD models to predict dispersion in ventilated spaces. Kassomenos et al. identified spatial variation in airborne vinyl chloride monomer (VCM) from poly vinyl chloride manufacture. In a mock up airliner cabin Zhang et al.[13] found that predictions of sulphur hexafluoride tracer gas concentration and airflow did not agree as well with the measured data as did predictions of air temperature. Convective transport of a gaseous contaminant is often based on the assumption that the contaminant will transport at the same rate as the air velocity. Turbulent flux is treated as an ensemble average of the combined contaminant and air velocity fluctuation and eddy diffusion coefficients are used in the Navier-Stokes equations as turbulence closure parameters. Chaouat and Schietsel[14] concluded that additional diffusion terms need to be approximated and applied to Large Eddy Simulation CFD models under conditions of non-homogenous turbulence. Eddy diffusion coefficient values were often not defined in these studies and were not specified as either being constant or variable. In the large scale atmosphere, effective diffusivity was proposed by Haynes and Shuckburgh[15] as a 'mixing diagnostic' where low effective diffusivity values identify areas of poor mixing.

The aim of the present investigation is to assess the variability in empirically estimated diffusivity of volatile organic carbon (VOC) vapour in a ventilated workroom to identify areas of poor mixing hence poor ventilation and increased occupational exposure risk. Air velocities and mass transfer coefficient values are also compared and implications of

variability in these parameters for dispersion prediction modeling are discussed. VOC vapour emissions from sources of relatively low and high volatility were investigated under typical workroom air velocities produced by two dilution ventilation supply rates. To deal with the difficulty in establishing a value for the effective diffusivity, this was estimated following the procedure proposed by Nakamura[16] and Chock et al.[17] whereby each Eularian division in space and time presents a new average gradient of transport across that division.

Design of the experimental space and determination of empirical effective diffusivities and mass transfer coefficient values.

Before undertaking the experimental measurements it was necessary to design the 40 m^3 experimental space by creating a grid representation for locating the measurement sensors. Average airborne vapour concentrations and steady state air velocities were measured at equivalent Eularian grid nodes with a distance between nodes of 0.4 to 0.5m along each Cartesian axis from the centre of the vapour source. Measurements (made as described in the experimental section) were recorded at ten minute intervals to provide data for every second over a 30s duration for the VOC vapour concentration and over a three minute period for the air velocity. A series of effective diffusivities were estimated based on the hypothesis that each Eularian division in space and time presents a new average gradient of transport across that division. Within each division in time it is assumed that the airflow and vapour concentration are at a steady state hence effective diffusivities are estimated over a quasi stationary spectrum (a snapshot in time) over space. This follows the 'frozen turbulence' hypothesis first proposed by Taylor[18]. Models of uniform, isotropic diffusion from a point source created for indoor air such as those by Wadden et al.[19] and Kreil et al.[20], were developed from Fick's laws[21]. Using Fick's diffusion equation in the one dimensional convection - diffusion 'general transport equation', the diffusion coefficient is redefined as 'effective diffusivity'. Following Nakamuru[16] and Shuckborugh and Haynes[22], effective diffusivity is therefore considered as the coefficient of proportionality attributed to a net dispersion driven by molecular diffusion, mixing by small scale turbulence and convection. Correlations between empirical effective diffusivity, mass transfer coefficient values, vapour concentration and air velocity data are required to be assessed.

Airborne vapour concentrations measured as described below were used in Fick's diffusion equation, equation (1), to estimate the effective diffusivity values.

$$\frac{\partial Cx}{\partial t} = Kx_i \frac{\partial^2 Cx}{\partial x^2} \quad (1)$$

Cx (mg m^{-3}) is the concentration of the diffusing substance at position i on the x axis measured at time t (s). The second differential term in the right hand side of equation (1) was estimated across three adjacent grid nodes by forward difference. Approximation by forward difference is considered reasonable when assuming that net migration of vapour is away from the source. For each relative rate of change in concentration with distance there may be three rates of change in concentration with time. The vapour concentration flux, $\partial Cx / \partial t$, estimated at the mid distance on the same Eularian grid, was treated as a fixed point value. The average effective diffusivity, Kx_i (m^2 s^{-1}) was therefore estimated and assigned to the mid distance on the Eularian grid; x_{i-1}, x_i, x_{i+1}. Effective diffusivities Ky_i and Kz_i were likewise determined across the corresponding one dimensional y and z axes.

The empirical effective diffusivities were used in the one dimensional convection – diffusion model, equation (2) to estimate VOC vapour mass transfer coefficient values at each of the Eularian grid nodes along the Cartesian axes.

$$\frac{\partial Cx}{\partial t} = Kx_i \frac{\partial^2 Cx}{\partial x^2} - u_{ci} \frac{\partial Cx}{\partial x} \quad (2)$$

and rearranging to give

$$u_{ci} = \left(\frac{\partial Cx}{\partial x}\right)^{-1} \left(-\frac{\partial Cx}{\partial t} + Kx_i \frac{\partial^2 Cx}{\partial x^2}\right) \quad (3)$$

Where u_{ci}, v_{ci} and ω_{ci} are the airborne vapour mass transfer coefficient values on the respective x, y and z axis at position i and time j and are compared to measured average air velocities at equivalent time and space nodes along the Cartesian axes. The effective diffusivity and mass transfer coefficient values for n- butyl ethanoate and methylbenzene were estimated under the experimental conditions described below.

Experimental procedure

In separate experiments, pure n-butyl ethanoate (NBE) and methylbenzene (MB) liquid (Fisher Scientific, Leics., UK) were placed in a small tray at the centre of the floor of the windowless rectangular room of $40m^3$ shown schematically in Figure 1. These solvents, commonly used in the surface finishing industry, were selected for their differences in

volatility, the standard ambient vapour pressure of NBE is 12 kPa and of MB is 29.5 kPa, NIOSH – ICSC:0399 and 0078[23]. Typical workroom air velocities ranging from 0.02 to 2.0 m s^{-1} were produced from a Fischbach® shell fan under two dilution ventilation supply rates of 0.1 and 0.23 m^3 s^{-1}. The fan was situated at half height of an open door. The outlet vent was the natural ventilation of an open door opposite the fan inlet. Average air velocity and velocity fluctuation were measured over three minutes at each grid node according to BS EN 13182:2002 (E)[24] using a calibrated omni directional hot sphere (OHS) anemometer, model 54N50 Dantec Dynamics®. The average airborne VOC vapour concentrations (ppm) were measured over 30 seconds at equivalent grid nodes to the air velocity measurements using mixed metal oxide semiconductor (MMOS) sensors, CityTechnology®. The MMOS sensors were calibrated daily in an airtight 1 m^3 container over the concentration ranges given in Table 1. The required volume of liquid solvent was injected through a septum seal and the vapour mixed to a homogenous concentration using a small fan which was sealed inside the cube. A total of 12 calibrated sensors were available for simultaneous measurement along the Cartesian axes (*dx* and *dy* of 0.4 to 0.8 m and *dz* of 0.25 to 0.5 m) after 10 and 20 minutes evaporation of the selected VOC in the 40 m^3 room. The sensors were capped to prevent exposure to solvent vapour prior to the required measurement time. It took a maximum of 30 seconds to remove all caps using a long, narrow metal hook to minimize any disturbance of the airflow field. As the sensors had a maximum response time of 30 seconds the VOC vapour concentration was estimated from the sensor output 15 seconds before and 15 seconds after the measurement time point. Room temperature, pressure and humidity conditions were recorded for conversion of vapour concentration from ppm to mg m^{-3}. Sensor array positions in the room, ventilation and solvent source position are illustrated in Figure 1.

Table 1. NBE & MB vapour concentrations for MMOS sensor calibration

Vapour Concentration (ppm)	**R^2 median (range)**
Bulk air: 10, 30, 50, 80, 100	0.989 (0.838 – 1.000)
Over the source: (z 0.25m) 100, 200, 300, 400	0.975 (0.966 – 0.991)

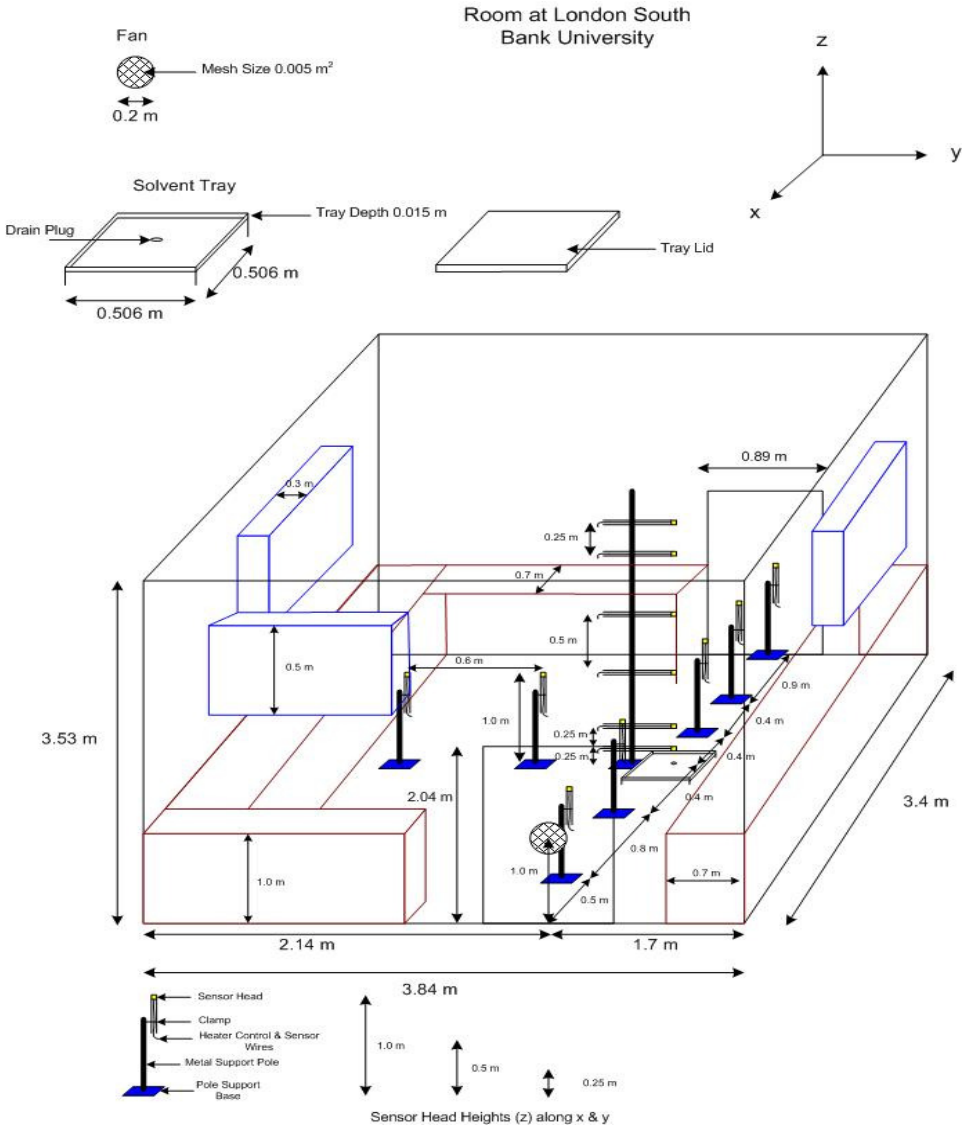

Figure 1. Room of 40 m^3* volume, dilution ventilation & MMOS sensor measurement layout. *Exact volume = room (46.09 m^3) – cabinets (6.59 m^3) = 39.5 m^3. © V.Hilborne

The NBE and MB vapour concentrations measured over time and space were used in equations (1) and (2) to estimate their respective empirical mass transport coefficient values in the ventilated room. Correlation between these values and air velocity at equivalent or adjacent grid nodes was assessed.

Measured values of effective diffusivity, mass transfer coefficient & air velocity.

The lower air input rate of 0.1 m^3 s^{-1} produced bulk air velocities ranging from 0.02 to 0.2 m s^{-1} with an air velocity of 3.5 m s^{-1} at the centre of the fan face. At the higher input rate of

0.23 m^3 s^{-1} the bulk air velocities ranged from 0.2 to 2.0 m s^{-1}, with a velocity of 8 m s^{-1} at the centre of the fan. NBE and MB vapour effective diffusivities and mass transfer coefficient values along the Cartesian axes, at the two air supply rates are given in Table 2. The majority of the estimated effective diffusivities values were at the middle of the given ranges whereas the mass transfer coefficient values tended toward the higher end of the range, particularly on the x axis close to the fan outlet. The maximum error (uncertainty) in vapour concentration measurement was ±13%. As concentration measurement is likely to be the greatest source of error it follows that the uncertainty in the empirically estimated effective diffusivity and mass transfer coefficient values would also be of the order of ±13%. Effective diffusivities, mass transfer coefficient values and air velocities are illustrated at equivalent Eularian grid nodes on the vertical z axis and horizontal x axis in Figure 2 (a - h). The x axis is considered the direction of airflow from the fan outlet to the vent. On the y axis, the horizontal axis perpendicular to the main airflow direction, the airborne vapour concentration was measured at only three grid nodes allowing for estimation of a single effective diffusivity for that axis. Effective diffusivities and mass transfer coefficient values for the y axis are given in Table 3. The illustrations in Figure 2 (a – c and e - g) clearly show that effective diffusivity and mass transfer coefficient vary with distance from the source over time. With air supply rate of 0.1 m^3 s^{-1} the NBE diffusivity profile was uniformly low along the entire z axis during the first 10 minutes evaporation. After 20 minutes evaporation, diffusivities close to the source dropped further while simultaneously increasing with distance. In contrast, under the same air supply rate the diffusivities of MB increased close to the source and decreased with distance over time. At the higher air input rate of 0.23 m^3 s^{-1} the NBE effective diffusivity values oscillate across the x axis with a drop in amplitude after 20 minutes. There was no evidence of any correlation between air velocity (including velocity fluctuation) and vapour concentration, mass transfer coefficient or effective diffusivity. For comparison, mean and standard deviation air velocities across the x and z axes are illustrated in Figure 2 (d and h). Estimated linear correlation coefficient between vapour mass transfer for all vapour species and air velocity at equivalent grid nodes ranged from 0.439 to 0.027 and the polynomial correlation ranged from 0.557 to 0.089. There was however a clear relationship between effective diffusivity and airborne vapour concentration. Where the vapour concentration was high, the effective diffusivity was low and vice versa. A steep change in vapour concentration over space and time is matched with little if any change in lower effective diffusivity values.

Table 2. Range in empirical effective diffusivities and mass transfer coefficient values of n-butyl ethanoate and methylbenzene vapours in the ventilated workroom under two air supply rates of 0.1 $m^3 s^{-1}$ and 0.23 $m^3 s^{-1}$.

VOC	**air supply ($m^3 s^{-1}$)**	**effective diffusivity ($m^2 s^{-1}$)**	**mass transfer coefficient ($m s^{-1}$)**
NBE	0.1	3×10^{-6} to 8×10^{-3}	3×10^{-6} to 2.5×10^{-2}
NBE	0.23	5×10^{-5} to 5×10^{-3}	5×10^{-5} to 1×10^{-2}
MB	0.1	1.6×10^{-5} to 7×10^{-3}	2×10^{-4} to 2×10^{-2}

Table 3. Empirical effective diffusivities and mass transfer coefficient values of n-butyl ethanoate and methylbenzene vapours on the y axis in the ventilated workroom under two air supply rates of 0.1 $m^3 s^{-1}$ and 0.23 $m^3 s^{-1}$.

VOC	**air supply ($m^3 s^{-1}$)**	**effective diffusivity ($m^2 s^{-1}$)**		**mass transfer coefficient ($m s^{-1}$)**	
		600 s	**1200 s**	**600 s**	**1200 s**
NBE	0.1	2×10^{-3}	5.5×10^{-4}	2×10^{-3}	2.5×10^{-3}
NBE	0.23	1×10^{-3}	8×10^{-3}	3.6×10^{-3}	8×10^{-3}
MB	0.1	9×10^{-3}	2.5×10^{-3}	8×10^{-3}	1×10^{-3}

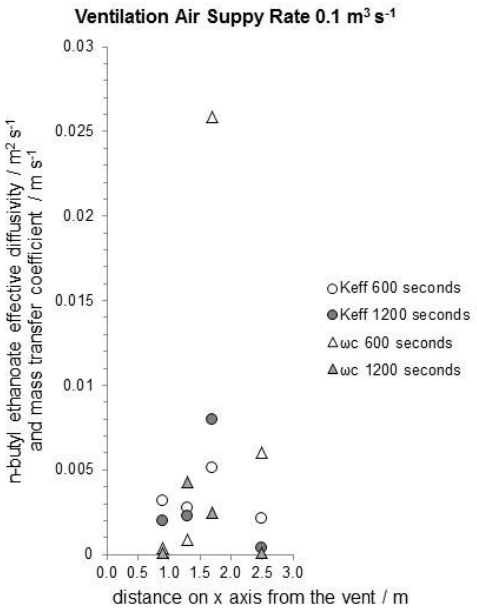
Ventilation Air Suppy Rate 0.1 m3 s-1
n-butyl ethanoate effective diffusivity / m2 s-1
and mass transfer coefficient / m s-1
Keff 600 seconds
Keff 1200 seconds
ωc 600 seconds
ωc 1200 seconds
distance on x axis from the vent / m

(a)

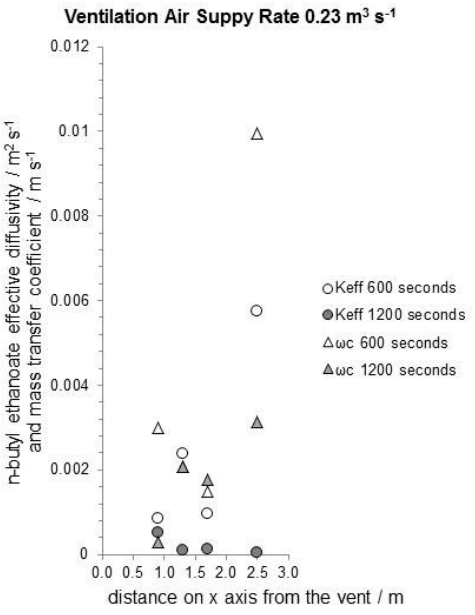
Ventilation Air Suppy Rate 0.23 m3 s-1
n-butyl ethanoate effective diffusivity / m2 s-1
and mass transfer coefficient / m s-1
Keff 600 seconds
Keff 1200 seconds
ωc 600 seconds
ωc 1200 seconds
distance on x axis from the vent / m

(b)

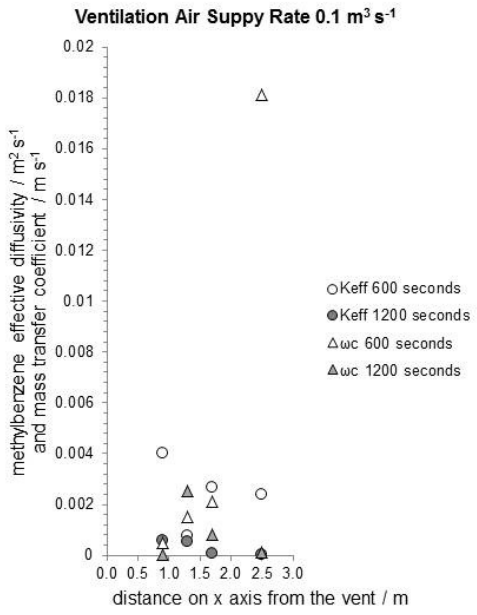
Ventilation Air Suppy Rate 0.1 m3 s-1
methylbenzene effective diffusivity / m2 s-1
and mass transfer coefficient / m s-1
Keff 600 seconds
Keff 1200 seconds
ωc 600 seconds
ωc 1200 seconds
distance on x axis from the vent / m

(c)

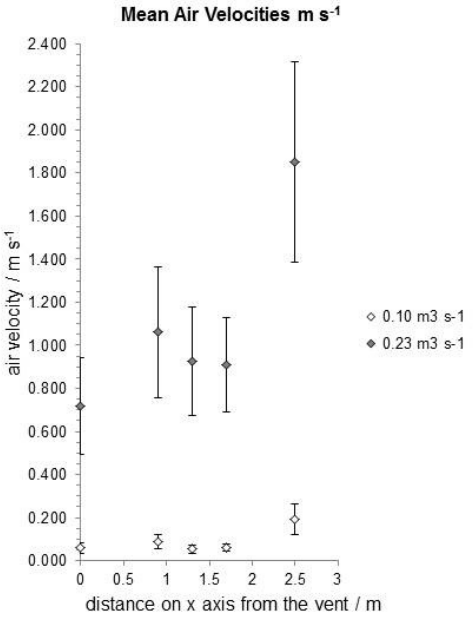
Mean Air Velocities m s-1
air velocity / m s-1
0.10 m3 s-1
0.23 m3 s-1
distance on x axis from the vent / m

(d)

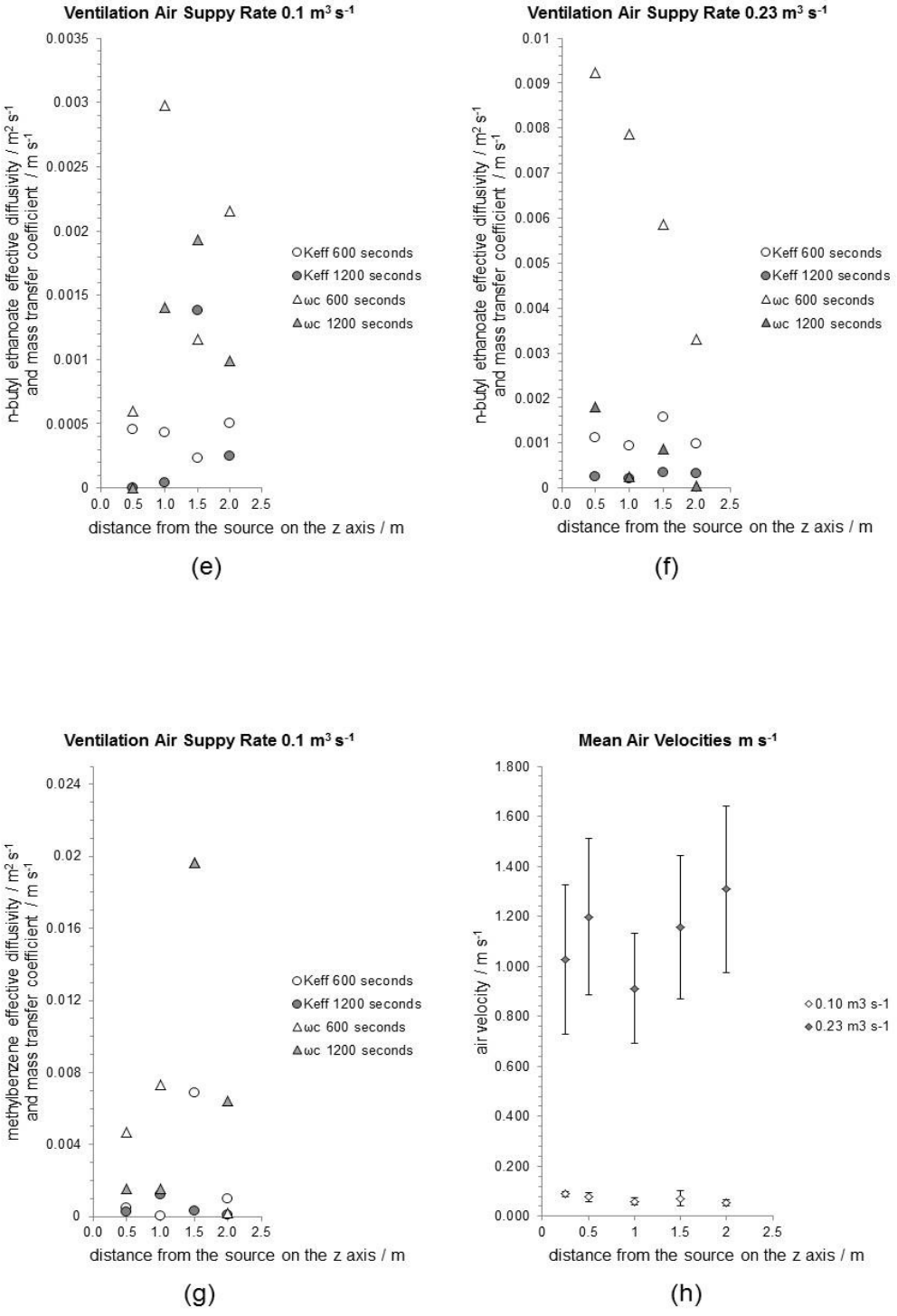

Figure 2 (a – c & e - g) Empirical effective diffusivities and mass transfer coefficient values of n-butyl ethanoate and methylbenzene vapors in the ventilated workroom under two air supply rates of 0.1 m^3 s^{-1} and 0.23 m^3 s^{-1}.(d & h) Air velocities at equivalent grid nodes. © V.Hilborne

Empirically estimated transport coefficient values of NBE and MB vapours along the Cartesian axes over time from a single source are clearly variable under typical workroom ventilation conditions. Consequently the use of these values in prediction modelling has implications for both accuracy and uncertainty in predicting vapour concentrations over time and space.

Using variable effective diffusivity & mass transfer coefficient in dispersion modelling.

The complexity in the flux, ebb and flow of air and pollutant transport over time and space is influenced by the type of ventilation used, including contributions from moving personnel and machinery. It is evident that the dispersion of airborne NBE and MB vapour from a source, under the applied ventilation conditions, is anisotropic. It is therefore likely that the ventilation efficiency varies across the room. Workers in large scale atmospheric dispersion modelling such as Degrazia et al.[25] and Goulart et al.[26] have established that the once assumed gradient K-theory with local turbulence closure should not be applied, particularly on the vertical z axis. From the variability in effective diffusivities of VOC vapours it follows that gradient transport should not be assumed along either of the Cartesian axes under the low air velocities typical to a ventilated workspace. The variability in effective diffusivity and mass transport values across space and time demonstrates the need for validation of the equivalent values estimated in transport prediction modelling. This is in agreement with Haghighat and Huang[27] who proposed an intermediate between CFD and 'well mixed' models called an integrated zonal model (IZM) and concluded that variable mass transfer coefficient values should be used for modelling dispersion in indoor air. Huang and Haghighat[28] compared an IZM model with a $k - \varepsilon$ CFD model presented by Murakami et al.[29]. Discrepancy in the VOC vapour profile was attributed to omission of turbulence diffusivity in the zonal model. Lack of correlation between air velocity, air velocity fluctuation and mass transfer coefficient questions the use of air velocities to estimate convective transport, particularly at the low air velocities typical to indoor spaces. Relationship identification would need further investigation as a correlation between air velocity and mass transfer should be proven exclusive of the use of eddy diffusivity or viscosity and mixing ratios for mass balance in predictive models.

Conclusions

Under the ventilation conditions and air velocities typical of an industrial workspace the dispersion of NBE and MB VOC vapours, from a single source, was anisotropic. Airborne vapour concentrations achieved steady state at only a few of the Eularian time and space grid nodes during the evaporation periods considered. This suggests that homogenous well mixed workspace air is unlikely to be achieved until a substantial period of time has passed. More detailed monitoring of vapour concentrations over time and space is therefore needed for realistic assessment of chronic exposure.

Effective diffusivity was used to describe net dispersion driven by molecular diffusion, mixing by small scale turbulence and convection over one dimension in space and time: gradients of dispersion were assumed across each grid node. Along each of the Cartesian axes from above the source, the respective empirical effective diffusivities and mass transfer coefficient values were variable. Variability in effective diffusivities confirms non - Fickian dispersion from the source along the length of the one dimensional axes. A clear correlation between vapour concentration and effective diffusivity was evident. When the vapour concentration was high, the diffusivity value was small indicating weak mixing and a barrier to transport. It followed that a high effective diffusivity value corresponded with a low vapour concentration indicating strong mixing. A correlation between air velocity and vapour transport data was not found suggesting that air velocity should not be used a-priori to represent mass transport.

The findings of this study demonstrate the variability in effective diffusivity and mass transport values of VOC vapours from a source in a dilution ventilated workspace. Areas of poor ventilation efficiency and periods of increased occupational exposure risk during surface treatment operations and equipment maintenance are highlighted by the low effective diffusivity values. These should be taken into account in order to comply with current legislation. Empirical estimation is recommended for validation of values applied in predictive models, such as numerical CFD. Increased knowledge of effective diffusivity of VOC vapours in ventilated air will support realistic occupational exposure risk assessment and improvement in ventilation design for workspaces used for surface coating, metal finishing and degreasing operations.

Acknowledgement

The authors would like to acknowledge the valuable help and advice given by the late Professor P. Nolan during the course of this work. Dr. Hilborne gives special thanks for his assistance and supervision during her Ph.D study.

References

1. HSE Engineering Information Sheet No EIS47. Solvent vapour degreasing plant. Use, maintenance and cleaning. March 2015.

2. A.F. Averill, J.M. Ingram and P.F. Nolan. Cleaning metal components after the Montreal Protocol – Introductory review. Trans. IMF, 1998, 76(3), 81-89.

3. A.F. Averill, J.M. Ingram and P.F. Nolan. After the Montreal Protocol – the right choice of cleaning system – part 1. Finishing, June 1998, 24-26.

4. A.F. Averill, J.M. Ingram and P.F. Nolan. On the performance and mechanism of ultrasonically cleaning metal components with environmentally acceptable organic solvents.Trans. IMF, 1999, 77(6), 230-236.

5. A.F. Averill, J.M. Ingram and P.F. Nolan. BCGA. Technical Report TR3. Replacement substances for the cleaning of oxygen system components. British Compressed Gases Association. (TR3). BCGA. 1999, ISSN 0260- 4809, 1-123.

6. J. Oliver. REACH – its implications for platers and coaters. Trans. IMF, 2008, 86(6), 292.

7. K. Hoare. What the new EU REACH regulation means for your business. Trans. IMF, 2009, 87(4), 170-172.

8. A.F. Averill, J.M. Ingram and P.F. Nolan. Replacing TCA and CFC-113 with HFE and HFC based azeotropes and n-propyl bromide based solvents for wipe cleaning metal components –source evaporation rates and models. Trans. IMF, 1999, 77(1), 16-26.

9. A.F. Averill, J.M. Ingram and P.F. Nolan. A study of the dispersion of solvent vapour in the workspace during wipe cleaning of metal components with organic solvents – a Monte Carlo uncertainty analysis. Trans. IMF, 1999, 77(5), 204-208.

10. R.B. Rood. Numerical advection algorithms and their role in atmospheric transport and chemistry models. Review of Geophysics, 1987, 25 (1), 71–100.

11. S.J. Emmerich and K.B. McGrattan. Application of a large eddy simulation model to study room air flow. ASHRAE Transactions, 1998, 104(1B), 1128-1137.

12. P. Kassomenos, A. Karayannis, I. Panagopoulos, S. Karakitsios and M. Petrakis. Modelling the dispersion of a toxic substance at a workplace. Environmental Modelling and Software, 2008, 23(1), 82–89.

13. Z. Zhang, X. Chen, S. Mazumdar, T. Zhang and Q. Chen. Experimental and numerical investigation of airflow and contaminant transport in an airliner cabin mock up. Building and Environment, 2009, 44, 85 – 94.

14. B. Chaouat and Schiestel R. From single-scale turbulence models to multiple scale and subgrid-scale models by Fourier transform. Theoretical Computational Fluid Dynamics, 2007, 21, 201–229.

15. P. Haynes and E. Shuckburgh. Effective diffusivity as a diagnostic of atmospheric transport. Journal of Geophysical Research, 2000, 105(D18), 22,777-810.

16. N. Nakamuru. Two dimensional mixing, edge formation and permeability diagnosed in area co-ordinates. Journal of the Atmospheric Sciences, 1996, 53, 1524-1537.

17. D.P. Chock, M.J. Whalen, S.L. Winkler and Pu Sun. Implementing the trajectory grid algorithm in an air quality model, Atmospheric Environment, 2005, 39(22), 4015-4023.

18. G.I. Taylor. The Present Position in the Theory of Statistical Diffusion, Advances in Geophysics, 1938, 6, 101-111.

19. R.A. Wadden, J.L. Hawkins, P.A. Scheff and J.E. Franke. Characterisation of emission factors related to source activity for trichloroethylene degreasing and chrome plating processes, Journal of the American Industrial Hygiene Association, 1991, 52, 349–356.

20. C.D. Kreil, D. Krupinski and M. Chamachkine. Eddy diffusivity measurements for exposure modelling, Paper 182, American Industrial Hygiene Conference and Exhibition, Dallas TX. 1997.

21. A. Fick. Uber Diffusion, Annalan der. Physik, Leipzig. 1855, 170(1), 59–86. London [Online] Available from: Wiley online library. Doi. 10.1002/andp.1855.1700.105. Accessed 29th June 2015.

22. E. Shuckburgh and P. Haynes. Diagnosing transport and mixing using a tracer based co-ordinate system, Physics of Fluids, 2003, 15(11), 3342–3357.

23. National Institute for Occupational Safety and Health (NIOSH) (2003), International Chemical Safety Cards (ICSC) Nos: 0399 & 0078, World Health Organisation (WHO), ILO, UNEP, EN. [Online]. Available from: http://www.cdc.gov/niosh/ipcs. Accessed 29th June 2015.

24. BS EN 13182:2002 Ventilation for Buildings – Instrumentation Requirements for Air Velocity Measurements in Ventilated Spaces, BSI 2002, 389 Chiswick High Road, London W4 4AL, UK.

25. G.A. Degrazia and D.M. Moriera. Derivation of an eddy diffusivity depending on source distance for vertically inhomogenous turbulence in a convective boundary layer, Journal of Applied Meteorology, 2001, 40, 1233–1240.

26. A.G. Goulart, D. Moreira, J.C. Carvalho and T. Tirabassi. Derivation of eddy diffusivities from an unsteady turbulence spectrum, Atmospheric Environment, 2004, 38(36), 6121–6124.

27. F. Haghigat and H. Huang. Integrated air quality model for prediction of VOC emissions from building materials, Building and Environment, 2003, 38(8),1007-1017.

28. H. Huang and F. Haghigat. An integrated zonal model for predicting indoor airflow, temperature and VOC distributions, American Society for Heating, Refrigeration and Air Conditioning Engineers (ASHRAE) Transactions, 2005, 111(1),601–611.

29. S. Murakami, S. Kato. K. Ito. Coupled analysis of TVOC emission and diffusion in a ventilated room by CFD, 2nd European conference on energy performance and indoor climate in buildings and 3rd international conference on indoor air quality, ventilation and energy conservation in buildings, EPIC'98, Lyon, France, 1998, 1, 19–26.